Theor Chem Acc (1997) 96:44–50

Theoretical
Chemistry Accounts

Electron correlation effects on the shape of the Kohn–Sham molecular orbital

Oleg V. Gritsenko, Evert Jan Baerends

Afdeling Theoretische Chemie, Vrije Universiteit, De Boelelaan 1083, 1081 HV Amsterdam, The Netherlands

Received: 11 December 1996 / Accepted: 10 January 1997

Abstract. Even systems in which strong electron correlation effects are present, such as the large near-degeneracy correlation in a dissociating electron pair bond exemplified by stretched H_2, are represented in the Kohn–Sham (KS) model of non-interacting electrons by a determinantal wavefunction built from the KS molecular orbitals. As a contribution to the discussion on the status and meaning of the KS orbitals we investigate, for the prototype system of H_2 at large bond distance, and also for a one-dimensional molecular model, how the electron correlation effects show up in the shape of the KS σ_g orbital. KS orbitals ϕ^{HL} and ϕ^{FCI} obtained from the correlated Heitler-London and full configuration interaction wavefunctions are compared to the orbital ϕ^{LCAO}, the traditional linear combination of atomic orbitals (LCAO) form of the (approximate) Hartree-Fock orbital. Electron correlation manifests itself in an essentially non-LCAO structure of the KS orbitals ϕ^{HL} and ϕ^{FCI} around the bond midpoint, which shows up particularly clearly in the Laplacian of the KS orbital. There are corresponding features in the kinetic energy density t_s of the KS system (a well around the bond midpoint) and in the one-electron KS potential v_s (a peak). The KS features are lacking in the Hartree-Fock orbital, in a minimal LCAO approximation as well as in the exact one.

Key words: Electronic structure theory of atoms and molecules – Density functional theory – One-electron model – Local kinetic energy and effective one-electron potential – Local effect of exchange and Coulomb correlation

1 Introduction

The Kohn-Sham (KS) approach [1] provides an efficient method for practical applications of density functional theory (DFT). As in other one-electron approaches, the orbitals $\phi_i(\vec{r})$ are defined within the KS theory through one-electron equations with an effective one-electron potential v_s, which is purely local in the KS case,

$$\left\{ -\frac{1}{2}\nabla^2 + v_s(\vec{r}) \right\} \phi_i(\vec{r}) = \epsilon_i \phi_i(\vec{r}), \tag{1}$$

and for the non-degenerate ground state of an N-electron system the N occupied KS orbitals yield the exact electron density $\rho(\vec{r})$

$$\sum_{i=1}^{N} |\phi_i(\vec{r})|^2 = \rho(\vec{r}). \tag{2}$$

However, in spite of their one-electron appearance, Eqs. (1) and (2) take electron correlation into account effectively. In cases where the electron correlation effects are strong, in the sense that the single-determinantal wavefunction of the Hartree-Fock (HF) model is a poor approximation to the exact wavefunction, the KS model system of noninteracting electrons is still described by a single determinant built from the KS orbitals. This raises the question: What is the status and meaning of the KS orbitals as compared to the HF orbitals? It has been argued [2–4] that the KS orbitals are physically meaningful, being solutions to a one-electron Hamiltonian describing an electron moving in the local KS potential $v_s(\vec{r})$ with the following components

$$v_s(\vec{r}) = v_{\mathrm{ext}}(\vec{r}) + v_H(\vec{r}) + v_{\mathrm{xc}}(\vec{r}), \tag{3}$$

The external (attraction by the nuclei) and Hartree (Coulomb repulsion by all electrons) potentials are the largest contributions in $v_s(\vec{r})$, which it shares with the Hartree-Fock "potential". The exchange-correlation potential $v_{\mathrm{xc}}(\vec{r})$ has as its largest contribution the potential due to the average Fermi hole, the exchange term in the HF operator being the potential of an orbital-dependent Fermi hole. The often noted similarity between the HF and KS orbitals can be explained immediately from the similarity between the KS and HF "potentials". However, there are subtle differences which arise from contributions to $v_{\mathrm{xc}}(\vec{r})$ that have no analogue in the HF operator, such as the potential of the Coulomb hole, and the so-called kinetic and response potentials, which we have discussed before [4–7]. It has,

Correspondence to: O.V. Gritsenko

for instance, been pointed out [8–10] that electron correlation, represented by the Coulomb hole potential, leads to contraction of the KS orbitals $\phi_i(\vec{r})$ around the nuclei as compared to the HF orbitals, which leads to a higher value of the kinetic energy T_s of the KS system as compared to the corresponding HF kinetic energy T^{HF}. One wonders if other correlation effects can be identified in the KS orbitals. A well-known case of strong correlation is the weak electron pair bond, exemplified by H_2 at large bond distance. Even in this case of strong mixing of the doubly excited determinant $|(\sigma_u)^2|$ with the HF determinant $|(\sigma_g)^2|$, the KS model still uses a single determinant for noninteracting electrons. In this paper we investigate whether and how the effect of electron correlation manifests itself in the shape of the σ_g KS orbital in this prototype case of strong near-degeneracy correlation.

Molecular orbitals are often represented with a linear combination of atomic orbitals (MO-LCAO), either in a minimal basis or with extended basis sets. In the case of the H_2 molecule at large bond distance R(H—H), the σ_g orbital of H_2 is represented within the minimal LCAO approximation simply as

$$\phi^{\mathrm{LCAO}}(\vec{r}) = \frac{1}{\sqrt{2+2S}}[a(\vec{r}) + b(\vec{r})], \tag{4}$$

where $a(\vec{r})$ and $b(\vec{r})$ are the $1s$ AOs of the H atoms A and B, and S is the overlap integral

$$S = \int a(\vec{r})b(\vec{r})\mathrm{d}\vec{r}. \tag{5}$$

We note that the HF σ_g orbital has the tendency for large R to become rather more diffuse around the H nuclei than the atomic $1s$ orbitals, but in a simple multiconfiguration self-consistent field (MCSCF) solution with just the $(\sigma_g)^2$ and $(\sigma_u)^2$ configurations, this will be corrected. We will compare accurate KS orbitals to the simple minimal basis MO-LCAO approximation (Eq. 4), which when squared provides the proper density $\rho(\vec{r})$ in the atomic regions of A and B, not the diffuse HF density. We note that the KS orbital cannot be expected to deviate from Eq. (4) significantly, if at all, in the atomic regions, but the ability of the MO-LCAO expansion form (Eq. 4) to describe the KS orbital in the bond midpoint region is not immediately evident.

In this paper accurate Kohn-Sham orbitals ϕ^{HL} and ϕ^{FCI} are obtained for the H_2 molecule at large bond distances from the correlated Heitler-London (HL) and full configuration interaction (FCI) wavefunctions. We also consider the case of a one-dimensional model of "two hydrogen-like atoms" discussed before by Perdew [11]. It will appear that the KS orbitals ϕ^{HL} and ϕ^{FCI} have an essentially non-LCAO structure, which shows up in particular in the behaviour of the Laplacian of ϕ_i around the bond midpoint. The corresponding kinetic energy density per particle, $-\frac{1}{2}\phi^*\nabla^2\phi/\rho$, has a well around the bond midpoint, which increases with the bond distance and which compensates the corresponding peak of the KS potential [5]. Contrary to this, the MO-LCAO expansion (4) lacks these features. The reasons for this difference will be elucidated by means of the one-dimensional model.

2 Results for H_2 and a one-dimensional molecular model

We shall demonstrate the bond-midpoint behaviour of the KS solution for the H_2 molecule. Writing an approximation for the single KS orbital of H_2 in the following general form,

$$\phi(\vec{r}) = \frac{1}{\sqrt{2(1+FS)}}\sqrt{a^2(\vec{r}) + 2Fa(\vec{r})b(\vec{r}) + b^2(\vec{r})}, \tag{6}$$

we note that with $F = 1$ $\phi(\vec{r})$ of Eq. (6) turns to the LCAO form ϕ^{LCAO} (Eq. 4), while with $F = S$ it represents the HL form ϕ^{HL}. When squared, ϕ^{HL} yields a density, which corresponds to the HL correlated wavefunction [12]

$$\Psi^{\mathrm{HL}}(\vec{x}_1, \vec{x}_2) = \frac{a^*(\vec{r}_1)b(\vec{r}_2) + a^*(\vec{r}_2)b(\vec{r}_1)}{2(1+S^2)^{\frac{1}{2}}} \times [\alpha(s_1)\beta(s_2) - \alpha(s_2)\beta(s_1)], \tag{7}$$

where $\{\vec{x}_i\} = \{\vec{r}_i, s_i\}$, $\{\vec{r}_i\}$ are the space and $\{s_i\}$ are the spin variables. Ψ^{HL} properly describes electron correlation in the H_2 molecule at large bond distances R(H—H). It is to be noted that the electron densities $|\phi(\vec{r})|^2$ of both forms of Eq. (6), with $F = 1$ and $F = S$, correctly reduce to the corresponding atomic densities $a^2(\vec{r})$ and $b^2(\vec{r})$ in the atomic regions of A and B.

Even at intermediate distances, an essentially accurate KS orbital can be obtained from FCI calculations of the ground state H_2:

$$\phi^{\mathrm{FCI}}(\vec{r}) = \sqrt{\frac{\rho^{\mathrm{FCI}}(\vec{r})}{2}}. \tag{8}$$

The density ρ^{FCI} in Eq. (8) has been obtained from FCI calculations in a basis with five s- and two p-type contracted Gaussian functions [5, 13, 14] and an extra d-type Gaussian with the exponent $\alpha = 1.0$ for each H atom. Characteristics of ϕ^{LCAO} and ϕ^{HL} will be compared with those of the accurate KS orbital ϕ^{FCI}. On a technical note we mention that care has to be taken to avoid spurious oscillations which may arise when obtaining HF or KS kinetic energy densities simply by taking second derivatives of the corresponding orbital when the latter is expanded in Gaussian basis functions. Due to the shape of the Gaussian basis functions, oscillations in the second derivative may arise even when the Gaussian representation of the orbital is everywhere close to the true (basis set-free) one. We will discuss this point, which has some relevance for the problem of obtaining accurate KS potentials from CI densities, elsewhere.

Qualitative features of the three-dimensional KS solution in the bonding region of H_2 are also reproduced with a one-dimensional model of two interacting "hydrogen-like atoms" [11]. In this model a single electron of the "atom" A is bound to the external delta-function potential $v_A = -\sqrt{2I}\delta(x)$, so that the atomic ionization energy is I and the "atomic" orbital is $a(x) = (2I)^{\frac{1}{4}}\exp(-(2I)^{\frac{1}{2}}|x|)$. Similarly, for the "atom" B the external potential is $v_B = -\sqrt{2I}\delta(x-R)$ and the atomic orbital is $b(x) = (2I)^{\frac{1}{4}}\exp(-\sqrt{2I}|x-R|)$, with R being

the bond distance. Within this model one can consider a one-dimensional analog ϕ^{1D} of the form (6)

$$\phi^{1D}(x) = \frac{1}{\sqrt{2(1+FS)}}\sqrt{a^2(x) + 2Fa(x)b(x) + b^2(x)} \quad (9)$$

where S is the overlap integral of the orbitals $a(x)$ and $b(x)$. With $F = 1$ Eq. (9) represents an analog ϕ^{1DLCAO} of the LCAO form (Eq. 4), while with $F = S$ it is an analog ϕ^{1DHL} of HL form.

In Fig. 1 the form of the orbitals $\phi^{LCAO}(\vec{r})$, $\phi^{HF}(\vec{r})$, $\phi^{HL}(\vec{r})$ and $\phi^{FCI}(\vec{r})$ is compared for the bond distance $R(\text{H—H}) = 5.0$ a.u. The orbitals are plotted as functions of the distance z from the bond midpoint. The HF model leads to an orbital that is rather more diffuse than the minimal LCAO orbital. It is lower at the nuclei and higher in the tails (not visible in the figure). This is a direct consequence of the unphysical behaviour of the Fermi hole in stretched H_2 [8, 10]. The other orbitals all have the same form and are rather close to each other. The largest difference observed is that between ϕ^{LCAO} on the one hand and ϕ^{HL}, ϕ^{FCI} on the other hand in the bond midpoint region.

In contrast to this, the Laplacian $\nabla^2\phi$ which yields the kinetic energy of the KS system has quite a different form for ϕ^{LCAO} and ϕ^{HL}, ϕ^{FCI} in the bond midpoint region. In order to illustrate this, in Fig. 2 values $\nabla^2\phi^{LCAO}$ and $\nabla^2\phi^{HL}$ are presented calculated at $R(\text{H—H}) = 10.0$ a.u. for points which are placed at the bond axis around the bond midpoint at $z = 0$. $\nabla^2\phi^{LCAO}$ is a monotonic function of z in this region and it exhibits a minimum at the bond midpoint. Contrary to this, $\nabla^2\phi^{HL}$ passes through symmetric local minima and reaches a local maximum at the bond midpoint.

This qualitatively different behaviour of the Laplacians has a spectacular effect on the corresponding kinetic energy densities $t_s(\vec{r})$:

$$t_s(\vec{r}) = -\frac{\phi^*\nabla^2\phi(\vec{r})}{2\rho(\vec{r})} = \frac{1}{8}\frac{(\nabla\rho)^2}{\rho^2} - \frac{1}{4}\frac{\nabla^2\rho}{\rho}. \quad (10)$$

In Fig. 3 t_s^{LCAO}, t_s^{HL} and t_s^{FCI} are plotted as functions of z for $R(\text{H—H}) = 5.0$ a.u. There is also plotted their one-dimensional analogue

$$t_s^{1D}(x) = -\frac{1}{2\phi(x)}\frac{d^2\phi(x)}{dx^2} = \frac{1}{8\rho^2(x)}\left(\frac{d\rho}{dx}\right)^2 - \frac{1}{4\rho(x)}\frac{d^2\rho}{dx^2}, \quad (11)$$

calculated with the HL form $\phi^{1DHL}(x)$ of Eq. (9) with $F = S$ and $I = 0.5$ a.u.

One can see from Fig. 3 that t_s^{LCAO} has a shallow form in the bond midpoint region. Contrary to this, t_s^{FCI}

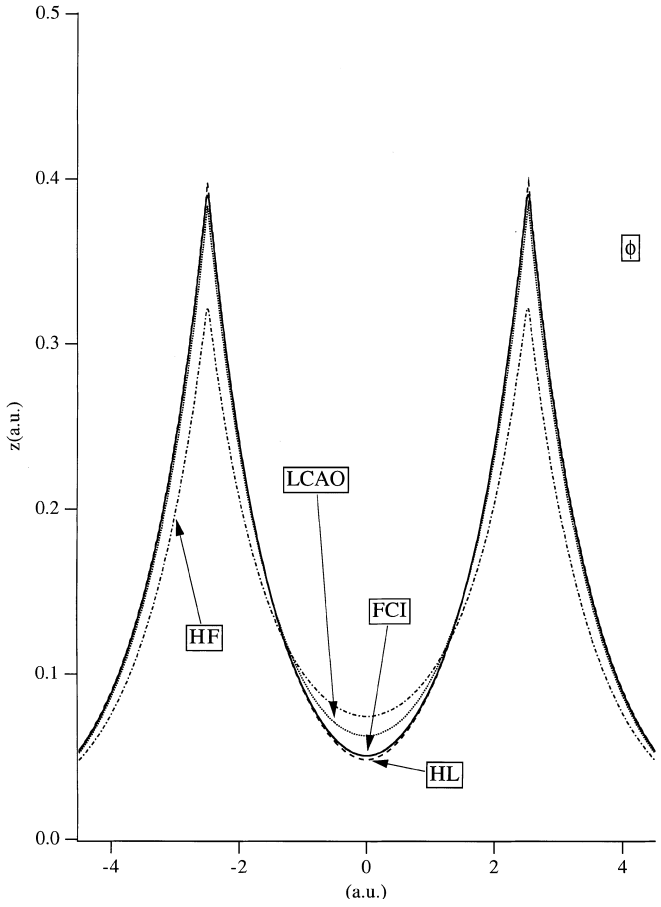

Fig. 1. Comparison of the HF σ_g molecular orbital and the full-CI (FCI), Heitler-London (HL) and LCAO Kohn-Sham orbitals for stretched H_2 (bond distance $R = 2$ bohr)

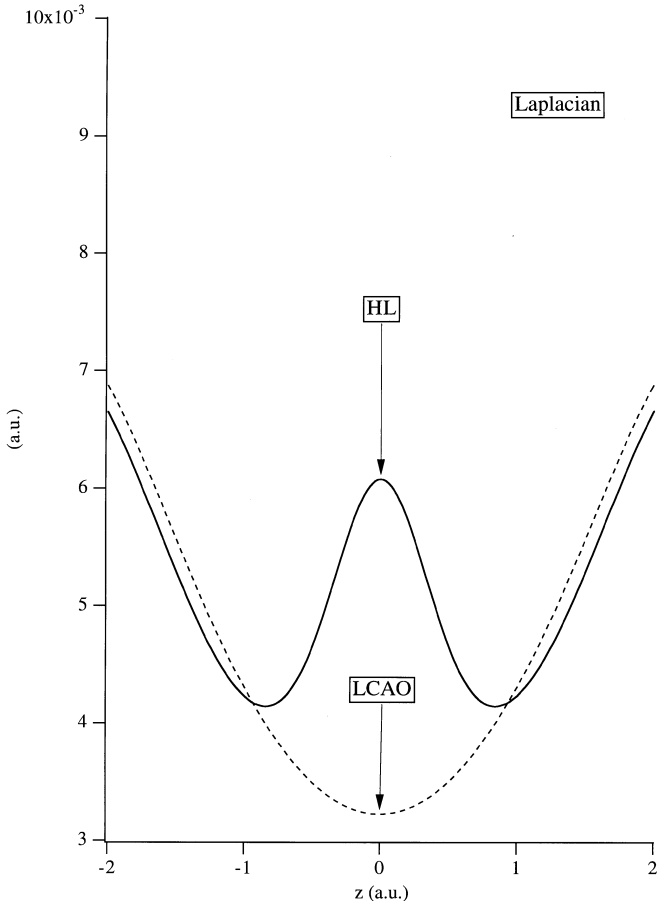

Fig. 2. Comparison of the Laplacians of the Heitler-London (HL) and LCAO Kohn-Sham orbitals around the bond midpoint for H_2 with bond distance $R = 10$ bohr

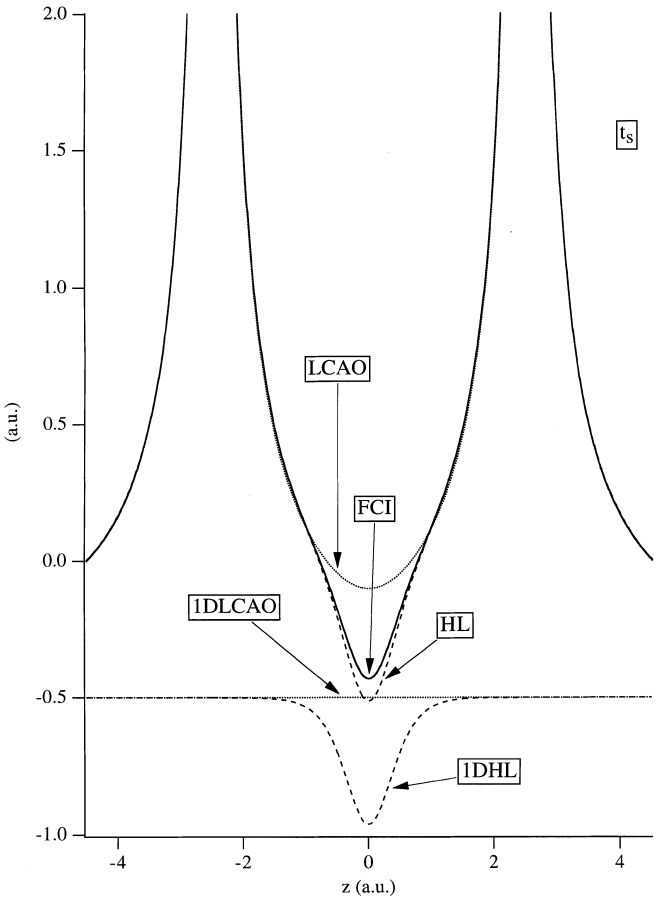

Fig. 3. Comparison of the FCI, HL and LCAO local Kohn-Sham kinetic energies for H_2 and the HL and LCAO ones for a one-dimensional model, for a bond distance of 5.0 a.u.

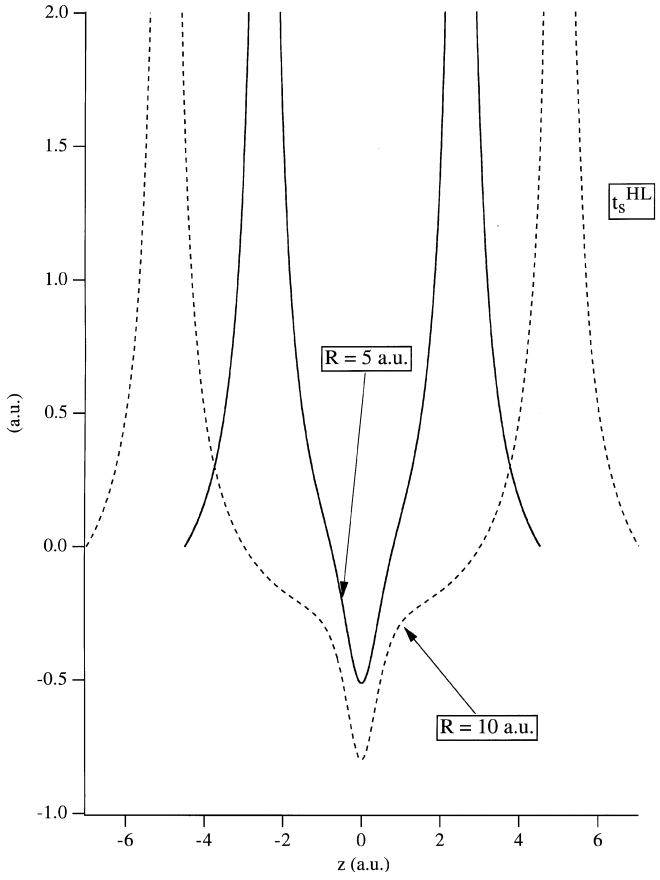

Fig. 4. Comparison of the HL local Kohn-Sham kinetic energies calculated for H_2 at the bond distances of 5.0 and 10.0 a.u.

and t_s^{HL} exhibit a characteristic feature of the KS solution, namely, a rather deep well of t_s around the bond midpoint. t_s^{FCI} and t_s^{HL} are close to each other for all z, so that the HL construction employed adequately reproduces, at this large bond distance, the correlation effect on the form of the KS solution. In the one-dimensional model this well of t_s is qualitatively reproduced by the one-dimensional analogue t_s^{1DHL}. While for the LCAO form $\phi^{\mathrm{1DLCAO}}(x)$ the corresponding kinetic energy density is a constant $t_s^{\mathrm{1DLCAO}}(x) \equiv -0.5$ a.u. (see below), t_s^{1DHL} exhibits a well around $z = 0$.

In Fig. 4 the functions t_s^{HL} are compared for $R(\mathrm{H—H}) = 5.0$ a.u. and $R(\mathrm{H—H}) = 10.0$ a.u. For both bond distances the characteristic features of t_s are singularities at the nuclei where t_s diverges and the above-mentioned well around the bond midpoint $z = 0$. The depth of the well increases with increasing bond distance and the minimum of t_s at the bond midpoint approaches for increasing bond distance the limiting value of twice the ionization energy: $t_s(z = 0) \to -2I = -1.0$ a.u.

The observed behaviour of the Laplacian of the KS orbital ϕ_s (either represented by ϕ^{HL} or by ϕ^{FCI}) around the bond midpoint, and the corresponding well of the KS kinetic energy density t_s, are a direct consequence of electron correlation effects. We may describe these effects in a simplified model by admitting configuration mixing of the HF $|(\sigma_g)^2|$ configuration with $|(\sigma_u)^2|$ to obtain the wavefunction

$$\Psi^{\mathrm{CI}} = c_g|\sigma_g\alpha(1)\sigma_g\beta(2)| + c_u|\sigma_u\alpha(1)\sigma_u\beta(2)| \tag{12}$$

yielding the KS orbital

$$\phi_s = \sqrt{\frac{1}{2}\rho} = \sqrt{c_g^2|\sigma_g|^2 + c_u^2|\sigma_u|^2}. \tag{13}$$

We use a minimal basis of atomic H 1s orbitals,

$$1s(\vec{r}) = \sqrt{\frac{\alpha^3}{\pi}}e^{-\alpha r}, \quad \alpha = \sqrt{2I} = 1.0, \tag{14}$$

so that in the limit of large distance R between the hydrogen atoms $S \to 0$, $c_g \to +1/\sqrt{2}$, $c_u \to -1/\sqrt{2}$, and Ψ^{CI} becomes identical to the HL wave function. An obvious difference between the σ_g and σ_u orbitals is that the σ_u has a node at the bond midpoint, M, so the configuration mixing reduces the density around M. This shows up in the lower values of the KS orbital around M compared to ϕ^{LCAO} in Fig. 1. For the behaviour of the Laplacian in the neighbourhood of M it is important that the first derivative with respect to z (taking the molecule to lie along the z-axis) of σ_u is nonzero (negative when giving $a(\vec{r})$ a positive sign in σ_u), all other first derivatives being zero:

$$\frac{\mathrm{d}}{\mathrm{d}z}\sigma_u(M) = -\sqrt{\frac{2+2S}{2-2S}}\,\sigma_g(M) \tag{15}$$

$$\frac{\mathrm{d}}{\mathrm{d}x}\sigma_u(M) = \frac{\mathrm{d}}{\mathrm{d}y}\sigma_u(M) = 0,\ \frac{\mathrm{d}}{\mathrm{d}x}\sigma_g(M) = \frac{\mathrm{d}}{\mathrm{d}y}\sigma_g(M) = \frac{\mathrm{d}}{\mathrm{d}z}\sigma_g(M) = 0. \tag{16}$$

The second derivatives for both σ_u and σ_g obey the relations

$$\frac{\mathrm{d}^2}{\mathrm{d}x^2}\sigma(M) = \frac{\mathrm{d}^2}{\mathrm{d}y^2}\sigma(M) = -\frac{2\alpha}{R}\sigma(M),\ \frac{\mathrm{d}^2}{\mathrm{d}z^2}\sigma(M) = \alpha^2\sigma(M). \tag{17}$$

For σ_g the saddlepoint at M is consistent with the positive "parallel" second derivative ($\mathrm{d}^2/\mathrm{d}z^2$) and negative "transverse" second derivatives ($\mathrm{d}^2/\mathrm{d}x^2$ and $\mathrm{d}^2/\mathrm{d}y^2$). All second derivatives are zero at M for the σ_u. For the Laplacian and kinetic energy density we obtain

$$t_s(M) = \frac{2\phi_s^*(-\frac{1}{2}\nabla^2)\phi_s}{\rho} = \frac{\left[-(c_g^2+c_u^2)\alpha^2 + \frac{4\alpha}{R}c_g^2\right]|\sigma_g(M)|^2}{2(c_g^2|\sigma_g(M)|^2 + c_u^2|\sigma_u(M)|^2)} = -\frac{\alpha^2}{2} + \frac{2\alpha}{R} - \frac{\alpha^2}{2}\left(\frac{c_u^2}{c_g^2}\right). \tag{18}$$

Without electron correlation ($c_u = 0$) the kinetic energy density is determined by the first two terms on the last line. The first term, due to the z-component of the Laplacian, has the value $-I = -0.5$ a.u. At the relatively large distance of 5 a.u., the second term, due to the x- and y-components of the Laplacian, still adds a correction of $+0.4$ a.u. to this term, leading to the much higher $t_s^{\mathrm{LCAO}}(M)$ of ca. -0.1 a.u. compared to the $-I = -0.5$ of $t_s^{\mathrm{1DLCAO}}(M)$ of the one-dimensional model. When R tends to infinity the "transverse components" of the Laplacian go to zero at M according to Eq. (18) and t_s of minimal LCAO H_2 will become equal to the -0.5 of the 1D model, where no transverse components exist. Electron correlation adds another $-\alpha^2/2 = -0.5$ multiplied by the factor c_u^2/c_g^2. This factor tends to 1 when the electron correlation becomes very strong at large distance. It is already rather large at $R = 5$ a.u., which explains the considerably lower values of $t_s^{\mathrm{FCI}}(M)$ and $t_s^{\mathrm{HL}}(M)$ in Fig. 3 than $t_s^{\mathrm{LCAO}}(M)$. The "correlation dip" in t_s, coming from the parallel component of the Laplacian, is in fact similar in the $1D$ model and in the H_2 case. It is the contribution of $+0.4$ a.u. at $R = 5$ bohr of the transverse components that shifts the $t_s(M)$ values of H_2 up with respect to the $1D$ model and makes them deviate from their limiting value at $R = \infty$ (-0.5 and -1 resp. for $t_s^{\mathrm{LCAO}}(M)$ and $t_s^{\mathrm{HL}}(M)$ resp.), but Fig. 4 demonstrates for $t_s^{\mathrm{HL}}(M)$ the tendency to approach the limiting value at $R = 10$ a.u.

The special correlation induced features that we have identified around the bond midpoint are very clear at large bond distances. One way wonder to what extent they show up at shorter distances, in particular the equilibrium bond distance. Figure 5a shows the Laplacians of the HF orbital and FCI KS orbital of H_2 at R_e. The difference is visible but not at all striking. Still, the correlation effects are present, but at R_e they are masked by the dominance of the large external (nuclear) and Hartree potentials, as may be seen from the relation

$$\frac{1}{2}\nabla^2\phi = (V_{\mathrm{ext}} + V_H + v_{\mathrm{xc}} - \epsilon)\phi. \tag{19}$$

In order to demonstrate that correlation effects, even if they are small, are definitely present we subtract our from $-t_s$ the large terms V_{ext} and V_H, which are at R_e very similar in the HF and FCI cases. Figure 5b shows plots of $-t_s - V_{\mathrm{ext}} - V_H$, which demonstrate that without the dominating nuclear and electronic coulombic potentials the correlation effects clearly show up. Note that Fig. 5b effectively compares, apart from the constant ϵ, v_{xc} and v_{x} in the KS and HF cases respectively.

In order to provide a solution of the one-electron Eq. (1), which requires that $-\frac{1}{2}\nabla^2\phi/\phi + v_s$ will be the constant ϵ also around the bond midpoint, a counterbalance to the well of t_s is developed in the KS potential, namely, the well-known bond midpoint peak v_s, which is known to become pronounced at large bond distance [5]. It clearly shows up in Fig. 6 if one compares v_s^{LCAO} to the potentials v_s^{HL} and v_s^{FCI}. These potentials are obtained at $R(\mathrm{H—H}) = 5.0$ a.u. by means of insertion of ϕ^{LCAO}, ϕ^{HL} and ϕ^{FCI} respectively into Eq. (1). The orbital energy ϵ in Eq. (1) is equal to minus the ionization energy of the system, which at large bond distances is

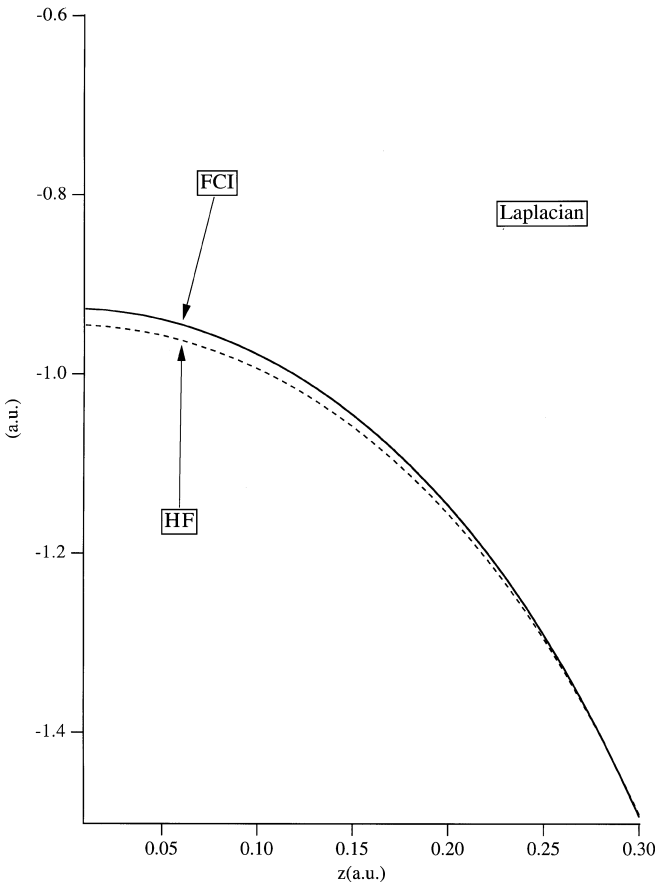

Fig. 5a. Laplacians of the Hartree-Fock and the full-CI Kohn-Sham orbitals for H_2 at equilibrium distance

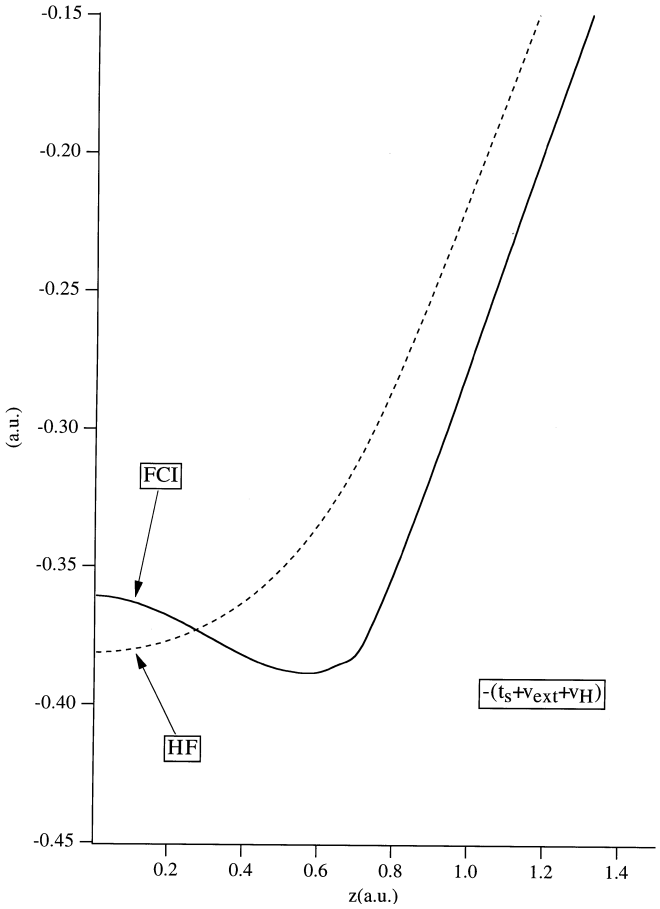

Fig. 5b. The Hartree-Fock kinetic energy density compared to the Kohn-Sham one (derived from a full-CI calculation), after subtraction of the external and Hartree potentials (see text), for H_2 at equilibrium distance

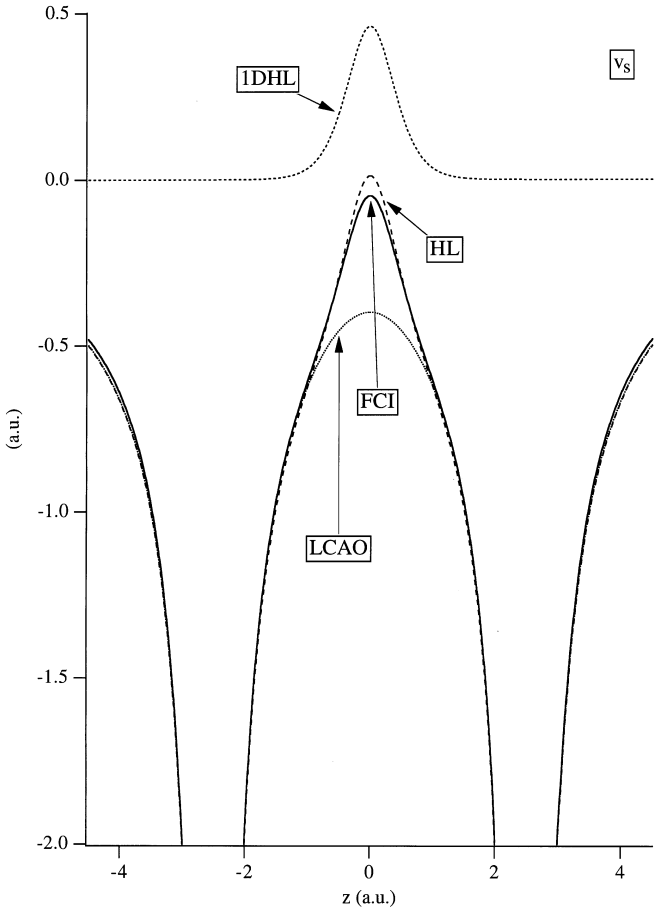

Fig. 6. Comparison of the Kohn-Sham potentials that reproduce the FCI, HL and LCAO electron densities for H_2 at 5 bohr and the HL one for a one-dimensional model

close to the atomic ionization energy $I = 0.5$ a.u. Taking this into account, we construct v_s^{LCAO} and v_s^{HL} with $\epsilon = -0.5$ a.u., while for v_s^{FCI} the value $\epsilon = -0.48$ a.u. is used, which has been obtained with the FCI calculations of H_2 and H_2^+ at $R(\mathrm{H{-}H}) = 5.0$ a.u. [5].

Figure 6 is essentially the counterpart of Fig. 3. v_s^{HL} and v_s^{FCI} possess a peak at the bond midpoint which compensates the well of t_s, while v_s^{LCAO} has a relatively shallow form. The effect looks even more spectacular for the one-dimensional potentials v_s^{1D}, which are constructed by the insertion of $\epsilon = -0.5$ a.u. and ϕ^{1DLCAO} or ϕ^{1DHL} into the one-dimensional analogue of the KS equation (1). v_s^{1DLCAO} is zero everywhere but at the nuclei, where, according to the construction, it turns to a delta-function. Contrary to this, v_s^{1DHL} exhibits a peak at the bond midpoint with the height of the peak being close to 0.5 a.u. (see Fig. 6).

Finally we note that the correlation-induced features in t_s around the bond midpoint are large at large bond distances, but because the density then becomes rather low in that region, the energetic effect is rather small. This would be different if the density were high in the region where the correlation effects occur. Such cases exist and will be examined in the future. It may be interesting to note that the less spectacular correlation-induced contraction of the electron density around the nuclei, which shows up in the considerably higher peaks of the KS orbital at the nuclei compared to the HF orbitals in Fig. 1, does have large energetic consequences, since it occurs in a region where the nuclear attraction potential and the electronic density are high. These consequences have been discussed before [8, 10].

3 Conclusions

We have shown that the KS molecular orbitals may exhibit features that are intimately related to the fact that these orbitals incorporate the effects of electron correlation. In the prototype case of near-degeneracy correlation, stretched H_2, the effect of strong admixture of the $|(\sigma_u)^2|$ configuration, or equivalently the use of the HL wavefunction, introduces special behaviour of the KS orbital around the bond midpoint. The special bond midpoint features of this KS orbital, as well as the related well of the KS kinetic energy density t_s, have been related to the striking bond midpoint peak of the KS potential v_s found earlier [5]. The peak of v_s has been derived from the "dynamical" properties of the conditional probability amplitude, describing the exchange

and Coulomb holes. These hole properties are absent from the HF wavefunction, but are built in by going to the HL wavefunction or by admixing of $|(\sigma_u)^2|$. Qualitative analysis and the results of calculations show that the depth of the t_s well and the height of the v_s peak increase with increasing bond distance, i.e. increasing configuration mixing, approaching the values $-2I$ and I, respectively, in the bond dissociation limit. One can expect similar effects in the bonding region whenever a weak covalent bond (large HF error) is present.

Being (up to a phase factor) the square root $\sqrt{\rho/2}$ of the correlated density ρ, the KS ϕ has an essentially non-LCAO form. Clearly, the minimal MO-LCAO form (Eq. 4) lacks the above-mentioned features around the bond midpoint. It is, of course, possible to build in these features by extending the basis set, since even with atom-centred basis sets a complete basis can in principle be constructed. Nevertheless, the MO-LCAO expansion is best suited to describe features in the atomic regions and one may expect a worse performance of the MO-LCAO expansion when it comes to representing features in the bond midpoint region. In the present case the correlation effects show up at large bond distance around the bond midpoint, i.e. in a region where the density is low, and the energy is not significantly affected. A traditional extended basis set will be able to provide a good approximation to the KS orbitals in the atomic regions and will not lead to significant errors in the energy of a KS calculation. However, a more definitive assessment of using traditional basis sets can only come from examining cases where strong configuration interaction leads to similar special effects in regions where the density is high.

References

1. Kohn W, Sham LJ (1965) Phys Rev 140A:1133
2. Baerends EJ, Gritsenko OV, van Leeuwen R (1996) In: Laird BB, Ross RB, Ziegler T (eds) Chemical applications of density functional theory. (ACS symposium series 629) p 20
3. Baerends EJ, Gritsenko OV, van Leeuwen R (1996) In: Tsipis CA, Popov VS, Herschbach DR, Avery JA (eds) New methods in quantum theory. (NATO ASI series 3, High technology, vol 8) Kluwer, Dordrecht, p 395
4. Gritsenko OV, Baerends EJ (1996) Phys Rev A54:1957
5. Buijse MA, Baerends EJ, Snijders JG (1989) Phys Rev A40:4190
6. Gritsenko OV, van Leeuwen R, Baerends EJ (1994) J Chem Phys 101:8955
7. Gritsenko OV, van Leeuwen R, Baerends EJ (1995) Phys Rev A52:1870
8. Buijse MA, Baerends EJ (1995) In: Ellis DE (ed) Density functional theory of molecules, clusters and solids. Kluwer, Dordrecht, p 1
9. Gritsenko OV, van Leeuwen R, Baerends EJ (1996) J Chem Phys 104:8535
10. Baerends EJ, Gritsenko OV, A quantum chemical view of density functional theory (to be published)
11. Perdew JP (1985) In: Dreizler RM, da Providencia J (eds) Density functional methods in physics (NATO ASI Series B123), Plenum Press, New York p. 265
12. Levine IN (1983) Quantum chemistry. Allyn and Bacon, Boston
13. Lie GC, Clementi E (1974) J Chem Phys 60:1275
14. Poirier R, Kari P, Csizmadia IG (1985) Handbook of Gaussian basis sets, Elsevier, Amsterdam